Rotman lens for mm-wavelengths

Leonard Hall[a], Hedley Hansen[b] and Derek Abbott[a]

[a]Centre for Biomedical Engineering and Department of Electrical and Electronic Engineering, The University of Adelaide, SA 5005 Australia
[b]Radar Division, DSTO, PO Box 1500, Edinburgh, SA 5111 Australia

ABSTRACT

The 77 GHz band has been reserved for intelligent cruise control in luxury cars and some public transport services in America and the United Kingdom. The Rotman lens offers a cheap and compact means to extend the single beam systems generally used, to fully functional beam staring arrangements.

Rotman lenses have been built for microwave frequencies with limited success. The flexibility of microstrip transmission lines and the advent of fast accurate simulation packages allow practical Rotman lenses to be designed at mm-wavelengths. This paper discusses the limitations of the conventional design approach and predicts the performance of a new Rotman lens designed at 77 GHz.

Keywords: Rotman lens, microstrip, mm-wavelengths, phased array

1. INTRODUCTION

Millimeter wave (mm-wave) radar systems are becoming an important part of the sensor suite for the next generation of automobiles and trucks. Applications include adaptive cruise control (ADC), forward and rear parking aids, and blind spot sensors. The latest generation of sensors operate in designated collision-avoidance bands at 24 or 77 GHz. The 24 GHz band is used by the high-resolution radar sensor developed by M/A-COM for short-range (< 20 meters) parking aid and blind-spot detection with a range resolution of a few centimeters, whereas 77 GHz is used for the adaptive cruise control sensor on the Mercedes S and E Class automobiles in Europe. These mm-wave radar sensors have significant advantages including increased range and detection performance over the ultrasonic sensors currently deployed as reverse parking aids.

Mercedes uses a system that switches rapidly among three beams by changing antenna feed points, creating a scanning effect inexpensively and with no moving parts. The beams are wide enough to ensure that each overlaps the adjacent beam, providing a combined 12-degree field of view. More advanced and expensive antenna systems rely on an antenna that is mechanically scanned and emits a narrow beam. The resolution is much higher than the three-beam system and has a larger scan angle. The increased mechanical complexity and size of the antenna makes this system unsuitable for this application.

This paper is concerned with the design and development of constrained lens solutions that address the limitations of current ADC systems. A Rotman lens built using microstrip techniques feeding a patch antenna array, offers an attractive alternative that provides high gain, large scan angles, conformal geometry, and low cost. The antenna array can scan in the same way the Mercedes system does. Instead of three beams the Rotman lens makes available many narrow, high gain beams, making the application of biologically inspired vision systems attractive.[1–4] Beam-width can be adjusted by combining adjacent beams to produce a broader beam with a lower gain. Scan angles of 60° and high gains are obtainable with careful design.

Further author information: (Send correspondence to L.T.Hall)
L.T.Hall: E-mail: lthall@eleceng.adelaide.edu.au, Telephone: (+61) 04 0233 6642
H. Hansen: E-mail: hedley.hansen@dsto.defence.gov.au
D.Abbott: E-mail: dabbott@eleceng.adelaide.edu.au

Smart Structures, Devices, and Systems, Erol C. Harvey, Derek Abbott, Vijay K. Varadan, Editors, Proceedings of SPIE Vol. 4935 (2002) © 2002 SPIE · 0277-786X/02/$15.00

2. DESCRIPTION OF ROTMAN LENS

A Rotman lens consists of a parallel plate region (body) with beam ports and array ports distributed along opposite contours. The central beam port provides equal path lengths to each array element. An offset beam port produces a path length difference and hence a phase gradient along an array, giving a steered beam.

The design of the lens is governed by the Rotman-Turner design equations[5] that are based on the geometry of the lens; these are shown in Fig. 1. The equations generate the positions of the antenna ports based on three perfect focal points (F_0, F_1, and F_2). The beam ports are placed on a circular arc joining the three focal points. The lower case letters represent their upper case variable normalised to the aperture size (maximum N), and w is the phase delay in wavelengths between the antenna port and patch antenna. The defining parameters of the Rotman lens are the internal scan angle α, ratio of $\frac{G}{F}$, value of f and the number of antenna ports (external scan angle).

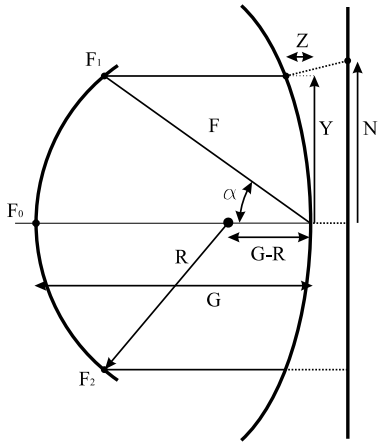

$$
\begin{aligned}
a &= \cos(\alpha) \\
b &= \sin(\alpha) \\
0 &= Aw^2 + Bw + C \\
A &= 1 - \frac{(g-1)^2}{(g-a)^2} - n^2 \\
B &= -2g - n^2b^2\frac{g-1}{(g-a)^2} + 2g\frac{g-1}{g-a} + 2n^2 \\
C &= -\frac{n^4b^4}{4(g-a)^2} + g\frac{n^2b^2}{g-a} - n^2 \\
R &= \frac{(Fa-G)^2 + F^2b^2}{2(G-Fa)}
\end{aligned}
$$

Fig. 1: Rotman Lens Topology[5]

3. ROTMAN LENS DESIGN, RULES OF THUMB

These rules of thumb have been used to quickly design cheap lenses for applications that do not require high levels of efficiency or gain. They tend to be applied to lenses with three to five beam ports with seven to fifteen antenna ports. These lenses can achieve approximately 10 dB sidelobes but they tend to suffer from poor isolation between ports and high sidelobes outside the scan angle due to reflections from the lens' side walls.

Typical rules of thumb are:

- $0.8 \leq f \leq 1$.
- Distance between ports[5] and antennas of $\leq \frac{\lambda}{2}$.
- Taper ports[6] with angle $\leq 12.5°$.
- Side walls have absorptive material or matched dummy ports.[6]
- Antenna lines are bent to implement required phase delays.[7–9]

4. HIGH PERFORMANCE ROTMAN LENS

We now summarize the design procedure for delivering high performance Rotman lenses.

A unique automation procedure that overcomes the time consuming fine tuning simulation that has hindered the deployment of efficient Rotman lens sensors. The automation of layout involves using Matlab to generate the lens design and exportation to DXF. This prepares the design for simulation (using Ensemble) or manufacture.

Historically reflections from the sidewalls are the biggest limiting factor affecting performance. Our approach has been to design sidewalls so that the reflected radiation within the lens is minimised. This involves evoking two sets of dummy ports, one, to deal with radiation from the antenna ports and the other to deal with the radiation from the beam ports. The orientation for well designed sidewalls is shown in Fig. 2. Little energy from the antenna ports will be incident on the beam dummy ports and the energy that does, is reflected directly onto the antenna dummy ports.

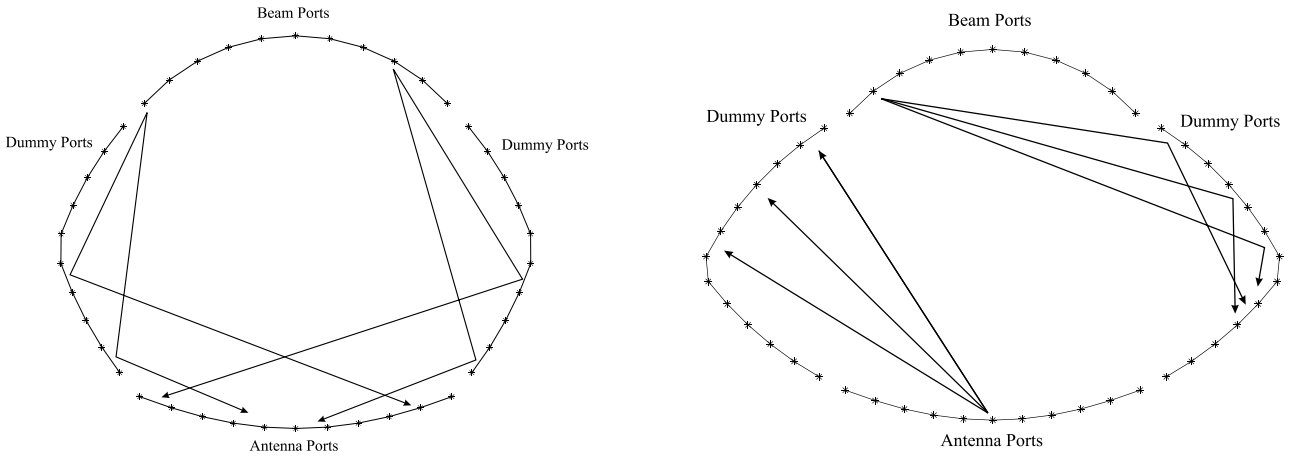

(a) Poorly Designed Sidewalls

(b) Well Designed Sidewalls

Fig. 2: Sidewall design

The S parameter impedance predictions are efficiently calculated using Ensemble software.

Port design and matching has been addressed by iteratively matching each port to the body of the lens then recalculating the S-matrix for the new port impedance. In addition, the challenge of shaping the fields around the port must be made to approximate those in the parallel plate region of the body of the lens. The tapered port rule of thumb, (see Section 3), works well.

An excitation taper has been introduced to minimise sidelobes by varying f. Fig. 3 shows the variation in shape of a Rotman lens as we vary f keeping the port spacing and aperture size constant. Fig. 3(b) and Fig. 3(c) show that keeping the half wavelength spacing between antenna ports becomes a problem after about $f = 0.75$ for the outer antenna ports. We have also maximised the beam-port widths for improving their isolation and for directing more energy towards the inner antenna ports. Although the width of a beam port is unable to be increased beyond $\lambda/2$, it is possible to excite two or more ports side by side to get an effective increase in port width.[10] By coupling two adjacent ports together a total gain of up to 3 dB is achieved and sidelobes are reduced by as much as 5 dB at the expense of slightly increased beam width.

Microstrip patch antennae are a feature of our approach. Beside the fact they provide low levels of mutual coupling, they most significantly radiate perpendicular to the surface they are mounted on. Since this allows the antenna to be displaced vertically without affecting performance in the horizontal plane, microstrip-lined constrained lens path lengths can be kept as straight as possible (is desired for avoiding electromagnetic discontinuities).[11–13]

5. FRONT END DESIGN

We propose the Rotman lens design shown in Fig. 4 for both transmit and receive sensing applications

The lens design shown in Fig. 4(a) has 29 antenna ports and 11 beam ports each made up of two subports. The patch columns in Fig. 4(b) are fed by a slot under the central patch and matched by an open ended stub.

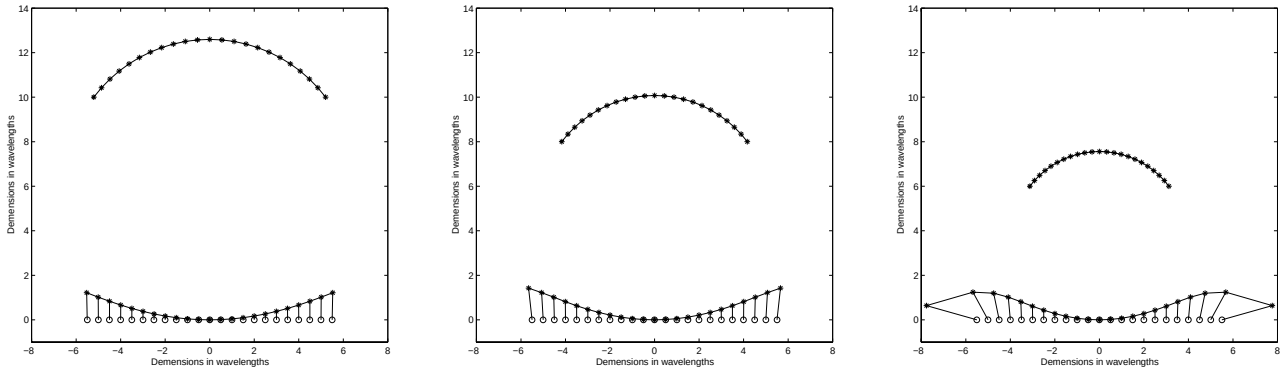

(a) $f = 1$ (b) $f = 0.8$ (c) $f = 0.6$

Fig. 3: Change in lens size and shape with f

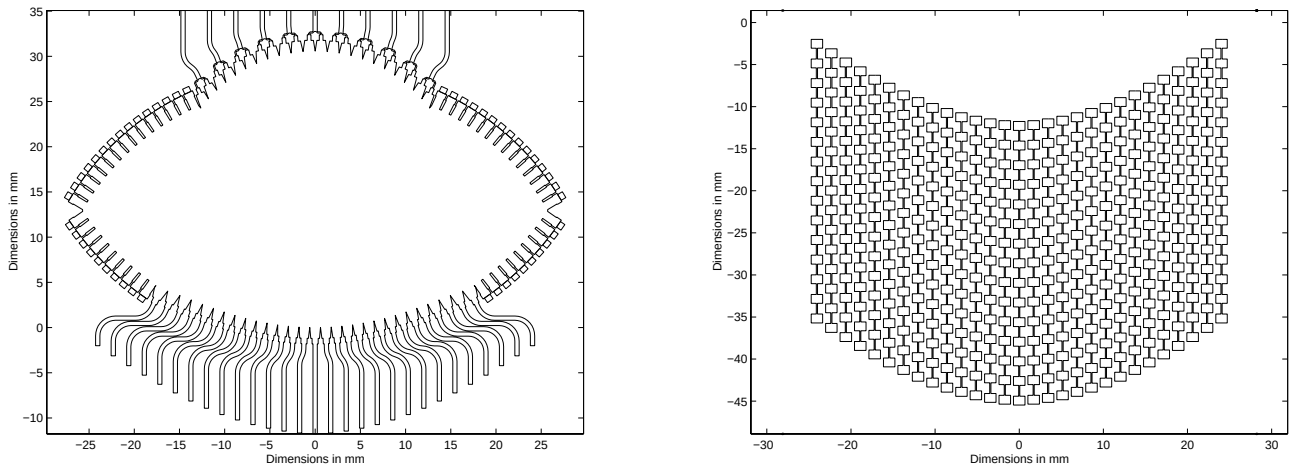

(a) Rotman Lens (b) Antenna Array

Fig. 4: Front end layout

This approach reduces the effect of frequency on beam pattern. The beam pattern for one side of the lens is shown in Fig. 5(a) and the patch columns in Fig. 5(b). Performance parameters are shown in Table 1. A feature of Fig. 5(a) is the low sidelobe levels.

Table 1: Predicted Lens Performance

Gain of Mainlobe	$>$ 25 dB
Beam Width	4°
Beam Crossover	-7 dB
Sidelobe	$<$ -15 dB
Total Insertion loss	$<$ 10 dB

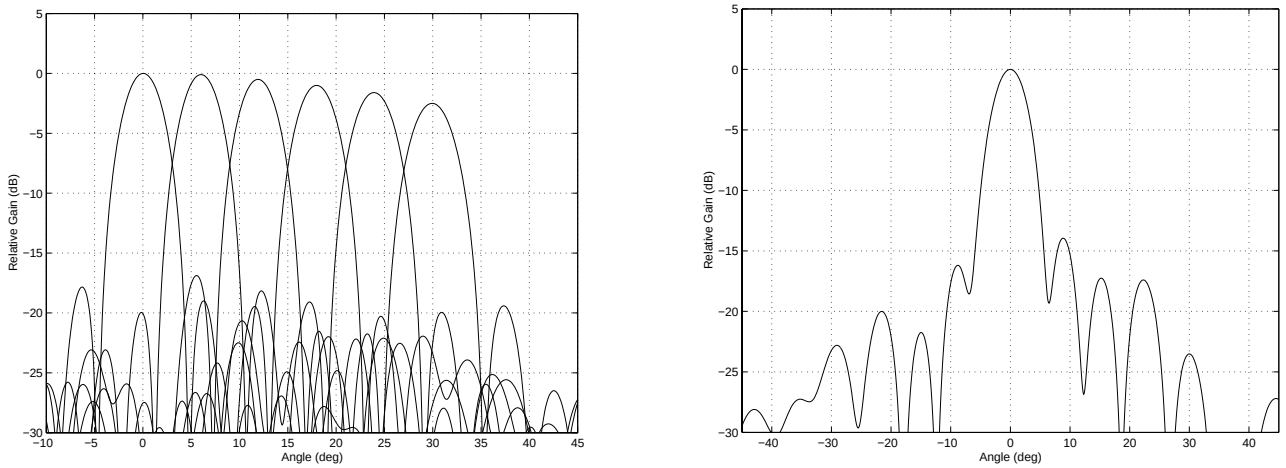

(a) Five Staring Beams

(b) Vertical Beam pattern

Fig. 5: Antenna Beam patterns

6. RADAR PERFORMANCE

The range for both clear weather (3.5 dB per/km attenuation) and poor weather (50 dB per/km attenuation) have been calculated using the following formula:

$R^4 = \frac{P_t G^2 \sigma \lambda^2}{(4\pi) kTBF_n (S_o/N_o) L_s}$.

Where the transmitted power P_t is 10 dBmW, radar cross section σ is 10 dBsm, wavelength λ is 3.89 mm, system noise figure F_n is 15 dB, detectable signal to noise ratio (S_o/N_o) is 7 dB, G is the antenna gain, kTB is the noise bandwidth product where B is 1 kHz and L_s is the loss in the system and is a combination of antenna loss and atmospheric loss.

The range at which a 10 dBsm target, in a sidelobe, will be detected has also been calculated. The results are calculated, using the antenna parameters presented in Table 1, and are shown in Table 2.

The performance characteristics outlined in this table are consistent with current state-of-the-art operating ADC systems. The substantial reduction in sidelobes when compared to work done by Metz[14] makes it possible to remove false targets by simply increasing the threshold for lower ranges. The improvements in scan angle over the system used by Mercedes means that automobile cut-in detection can be implemented with intelligent cruise control in the same system.

Table 2: Predicted Lens Performance

Range (clear weather)	> 120 m
Range (poor weather)	> 90 m
Sidelobe Range (clear weather)	< 50 m
Range Resolution	< 1m

7. CONCLUSION

This report demonstrates the feasibility of a planar 77 GHz beam staring antenna array as a front end for a collision avoidance system. The antenna array consists of serially fed microstrip patch elements arranged in columns and connected to a Rotman lens to realise a steerable antenna. An Epsilon Lambda Electronics Corporation 77 GHz FMCW radar connected as the back end to our Rotman lens promises both good range and wide scan angles.

ACKNOWLEDGMENTS

Funding from the DSTO RF Hub and the Sir Ross and Sir Keith Smith fund is gratefully acknowledged.

REFERENCES

1. A. Moini, A. Bouzerdoum, A. Yakovleff, D. Abbott, O. Kim, K. Eshraghian, and R. Bogner, "An analog implementation of early visual processing in insects," in *International Symposium on VLSI Technology, Systems, and Applications*, pp. 283–287, (Taipei), May 1993.
2. D. Abbott, A. Yakovleff, A. Moini, X. T. Nguyen, A. Blanksby, R. Beare, A. Beaumont-Smith, G. Kim, A. Bouzerdoum, R. E. Bogner, and K. Eshraghain, "Biologically inspired obstacle avoidance – a technology independent paradigm," in *Proc. SPIE Mobile Robots X*, **2591**, pp. 2–12, (Philadelphia), October 1995.
3. D. Abbott, A. Moini, A. Yakovleff, X. T. Nguyen, A. Blanksby, G. Kim, A. Bouzerdoum, R. E. Bogner, and K. Eshraghian, "A new VLSI smart sensor for collision avoidance inspired by insect vision," in *Proc. SPIE Intelligent Vehicle Highway Systems*, **2344**, pp. 105–115, (Boston), November 1995.
4. D. Goodfellow, G. P. Harmer, and D. Abbott, "mm-Wave collision avoidance sensors: future directions," in *Proc. SPIE Sensing and Controls with Intelligent Transportation Systems*, **3525**, pp. 352–362, 1998.
5. W. Rotman and R. F. Turner, "Wide angle microwave lens for line source applications," *IEEE Trans. Antennas Propag.* **AP-11**, pp. 623–632, November 1963.
6. L. Musa and M. S. Smith, "Microstrip port design and sidewall absorption for printed Rotman lenses," *Proc. IEE Proceedings Microwaves, Antennas and Propagation* **136**, pp. 53–58, Febuary 1989.
7. D. Abbott and A. Parfitt, "Collision avoidance device using passive millimetre-wave array based on insect vision," in *Proc. IREE 14th Australian Microelectronics Conference (Micro' 97)*, pp. 201–204, (Melbourne), October 1997.
8. D. Abbott and A. J. Parfitt, "Extension of the insect-vision paradigm to millimeter waves," in *Proc. SPIE Transportation Sensors*, **3207**, pp. 103–106, (Pittsburg), October 1998.
9. A. Mohamed, A. Campbell, D. Goodfellow, D. Abbott, H. Hansen, and K. Harvey, "Integrated millimetre wave antenna for early warning detection," in *Proc. SPIE Design, Characterization and Packaging for MEMS and Microelectronics*, **3893**, pp. 461–469, (Queensland), October 1999.
10. A. K. S. Fong and M. S. Smith, "A microstrip multiple beam forming lens," *radio and Elec.Eng* **54**, pp. 318–320, 1984.
11. L. Hall, D. Abbott, and H. Hansen, "Design and simulation of a high efficiency Rotman lens for mm-wave sensing applications," in *Proc. 2000 Asia Pacific Microwave Conference*, pp. 1419–1422, (Sydney), December 2000.
12. L. Hall, D. Abbott, and H. Hansen, "Microstrip-based Rotman lens for mm-wave sensing operations," *Passive Millimeter wave Technology V* **4373**, pp. 40–48, (Orlando), April 2001.

13. L. Hall, D. Abbott, and H. Hansen, "Monolithic fabrication of Rotman lenses," in *Monolithic fabrication of Rotman lenses*, **4593**, pp. 119–127, (Adelaide), December 2001.
14. C. Metz, J. Grubert, J. Heyen, A. Jacob, S. Janot, E. Lissel, G. Oberschmidt, and L. Stange, "Fully intergrated automotive radar sensor with versatile resolution," *IEEE Trans. Microwave* **49**, pp. 2560–2566, December 2001.